Opto-Electronic Science

Supplementary information
April 2023, Vol. 2, No. 4

DOI: 10.29026/oes.2023.230006

Hybrid bound states in the continuum in terahertz metasurfaces

Junxing Fan[1], Zuolong Li[2], Zhanqiang Xue[1], Hongyang Xing[1], Dan Lu[1], Guizhen Xu[1], Jianqiang Gu[2]*, Jiaguang Han[2,3]* and Longqing Cong[1]*

[1]Department of Electrical and Electronic Engineering, Southern University of Science and Technology, Shenzhen 518055, China; [2]Center for Terahertz Waves and College of Precision Instrument and Optoelectronics Engineering, Tianjin University, Tianjin 300072, China; [3]Guangxi Key Laboratory of Optoelectronic Information Processing, School of Optoelectronic Engineering, Guilin University of Electronic Technology, Guilin 541004, China.

*Correspondence: JQ Gu, E-mail: gjq@tju.edu.cn; JG Han, E-mail: jiaghan@tju.edu.cn; LQ Cong, Email: conglq@sustech.edu.cn

This file includes:

Supplementary information for this paper is available at https://doi.org/10.29026/oes.2023.230006

Section 1: Eigenvalues and quality factors for H_x-BIC supercell with asymmetric resonators

The intrinsic band folding operation was discussed in Fig. 2 in main text where all the resonators are symmetric and the band diagram was analyzed by artificially choosing unit cells. In real scenarios, H_x-BIC metasurface was constructed by displacing the gap of DSRR from center so that symmetry was broken in one resonator of the rectangular unit cell. The quality factors in H_x-BIC metasurfaces inherit the same band-folding properties as shown in supplementary Fig. S1(a) ($\alpha = 0.495\%$). The only difference with Fig. 2(e) is that BIC was degraded to a quasi-BIC due to the breaking symmetry in H_x-BIC supercell as revealed by the finite value of quality factor at Γ point. In addition, the coefficient of Q versus k relationship from U-qBIC to H_x-BIC supercell is no longer multiplied by 4 times, and ~4.5-time improvement of the coefficient is obtained due to the breaking symmetry, and an additional constant $B_{1/2}$ in the inverse quadratic equation is necessary to account for the asymmetry as shown in supplementary Fig. S1(b). Although three energy bands exhibit BIC characteristics (Fig. S1(a)), they basically originate from different mechanisms. The illustrated surface current distributions (Fig. S1(c)) based on simulations clearly present the mode patterns related to the three different resonances in Fig. 1(e). At 0.42 THz, these loop currents generate magnetic dipoles perpendicular to xy plane and are directed outward and inward for the left and right SRRs, respectively, whose interactions form a head-to-tail magnetic field. Such a configuration of current distributions is a characteristic feature of toroidal dipole, resulting in diminished far-field radiation[S1]. At 0.518 THz, the loop currents in the neighboring SRRs possess the same phase, and the individual SRR itself forms a diminished far-field radiation when asymmetry degree α becomes smaller which is the origin of symmetry-protected BIC. At 0.75 THz, the middle two arms of four branches in the two neighboring SRRs of a H_x-BIC superlattice constitute a loop current, generating a downward magnetic dipole. The arms in the edges also constitute a loop current with the neighboring supercells, generating an upward magnetic dipole. The upward and downward oriented magnetic dipoles form a toroidal dipole.

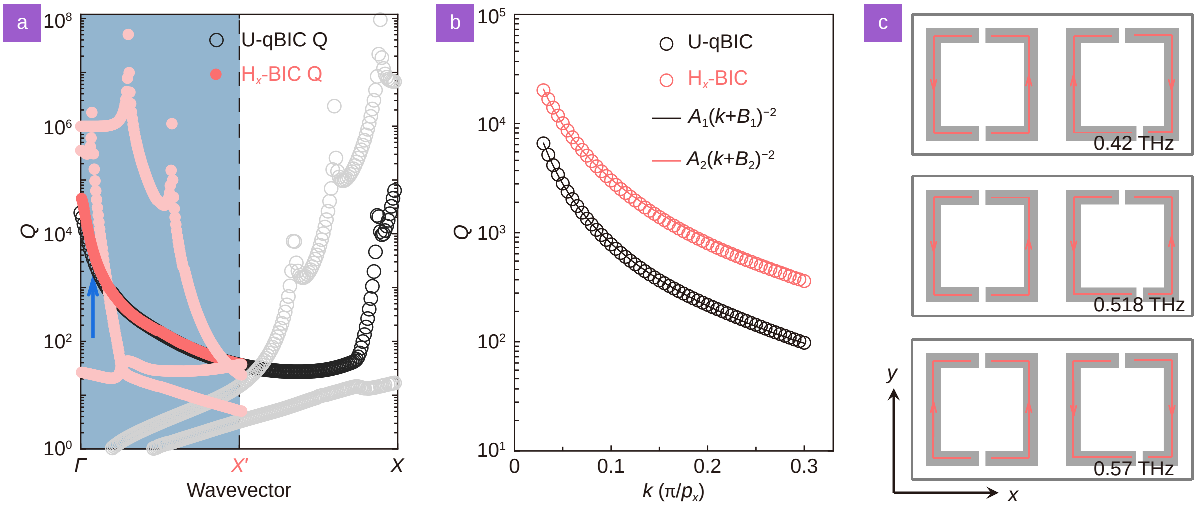

Fig. S1 | Folding of quality factors for H_x-BIC supercell with asymmetric resonators. (**a**) Quality factors of U-qBIC (black) and H_x-BIC (orange color) supercells at 0.495% asymmetry degree. (**b**) Radiative quality factors (circles) and corresponding fitting curves (solid lines). Here, A_1=9.485, A_2=43.108, B_1=0.07082, B_2=0.014. (**c**) Surface current distributions of H_x-BIC supercell in different resonances.

Section 2: H_y-BIC supercell

Similar to H_x-BIC supercell, the hybrid supercells along y-axis (H_y-BIC supercell) share the same band folding operation but from Γ-Y in the Brillouin zone as shown in supplementary Fig. S2. The calculated band diagram and the accompanying Q are shown in supplementary Fig. S2(c) and S2(d). The increase of quality factor in the hybrid BIC supercell was numerically and experimentally demonstrated in supplementary Fig. S2(e) and S2(f). The surface current of the relevant resonant mode in Fig. S2(f) is shown in Fig. S2(g).

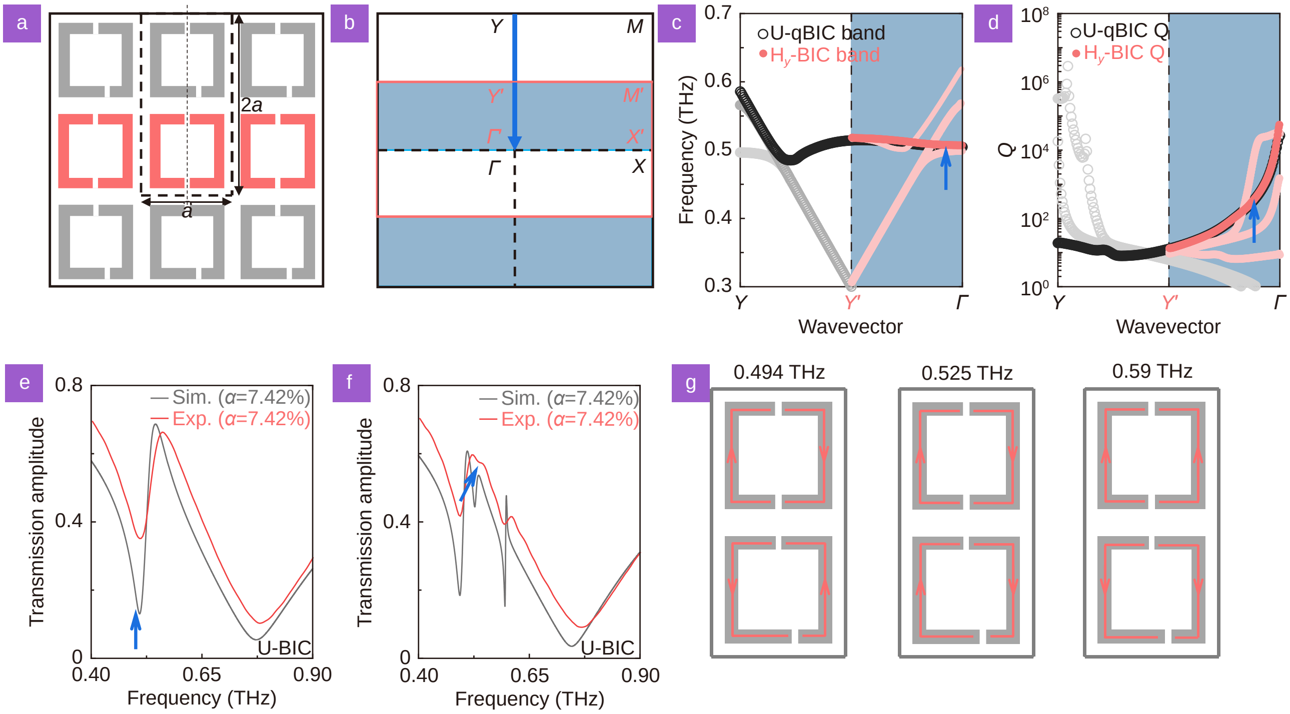

Fig. S2 | H_y-BIC supercell. (**a**) H_y-BIC metasurface with C_2 symmetry preserved in the neighboring resonators along *y*-axis in a supercell. (**b**) Band folding of H_y-BIC supercell from U-qBIC supercell. (**c**) Eigenvalues of U-qBIC (black circles) and H_y-BIC supercells (orange solid line). (**d**) Radiative *Q* of U-qBIC (black circles) and H_y-BIC supercells (orange solid line). (**e, f**) Simulated and experimental transmission amplitude spectra of U-qBIC and H_y-BIC metasurfaces with an asymmetry degree of 7.42%. (**g**) Surface current distributions of H_y-BIC supercell in different resonances.

Section 3: H_d-BIC supercell

Another similar operation as $H_{x/y}$-BIC supercell is by displacing the gap of resonators in diagonal direction in a unit cell (H_d-BIC) as shown in supplementary Fig. S3(a) that would extend the band folding operation to *Γ*-*M* in the BZ (Supplementary Fig. S3(b)). Exactly the same interpretation could be generalized to H_d-BIC supercell, and the simulated and experimental results verify the discussion (Supplementary Fig. S3(e) and S3(f)). The surface current of the relevant resonant mode in Fig. S3(f) is shown in Fig. S3(g).

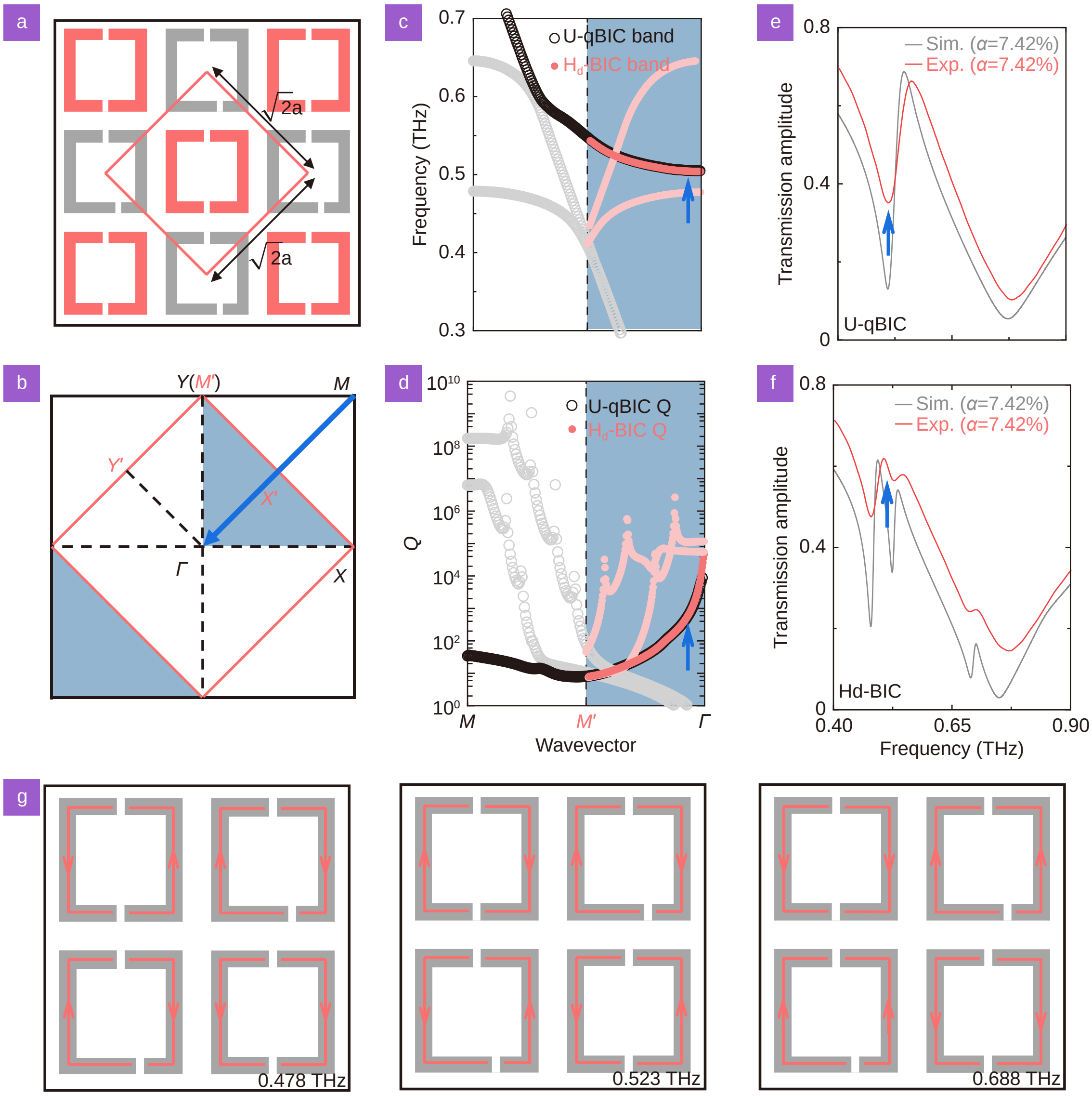

Fig. S3 | H_d-BIC supercell. (**a**) H_d-BIC supercell with C_2 symmetry preserved in the neighboring resonators along diagonal direction. (**b**) Band folding of H_d-BIC supercell along *Γ-M*. (**c**) Calculated eigenvalues of U-qBIC (black circles) and H_d-BIC supercells (orange lines). (**d**) Radiative quality factors of U-qBIC (black circles) and H_d-BIC supercells (orange lines). (**e, f**) Simulated and experimental transmission amplitude spectra of U-qBIC and H_d-BIC metasurfaces. (**g**) Surface current distributions of H_d-BIC supercell in different resonances.

Section 4: Radiative quality factors of H_t-BIC and H_q-BIC supercells

Radiative *Q* of H_t-BIC and H_Q-BIC supercells are shown in supplementary Fig. S4. Here quality factors of seven bands are shown with six bands folded from *X*, *Y*, and *M* points in U-qBIC supercell. Focusing on the original band highlighted by the arrow, a significant improvement of *Q* is observed in H_q-BIC near *Γ* point (supplementary Fig. S4(c)) due to a smaller number of radiative resonators. However, the divergent *Q* gradually merges far from *Γ* point where wave vector *k* plays a dominant role, and all the four resonators leak to a far field in the supercell.

Section 5: Resonances with fabrication imperfection

Resonance stability is of great importance to practical applications. We show the calculated transmission spectra of U-qBIC and H_x-BIC metasurfaces with round-angle resonators characterized by radius *r* as shown in supplementary Fig. S5. Such a rounded angle resonator is common in conventional lithography fabrication processes. The transmission spectra reveal that H_x-BIC supercell would guarantee a relatively larger and more stable quality factor than U-qBIC supercell.

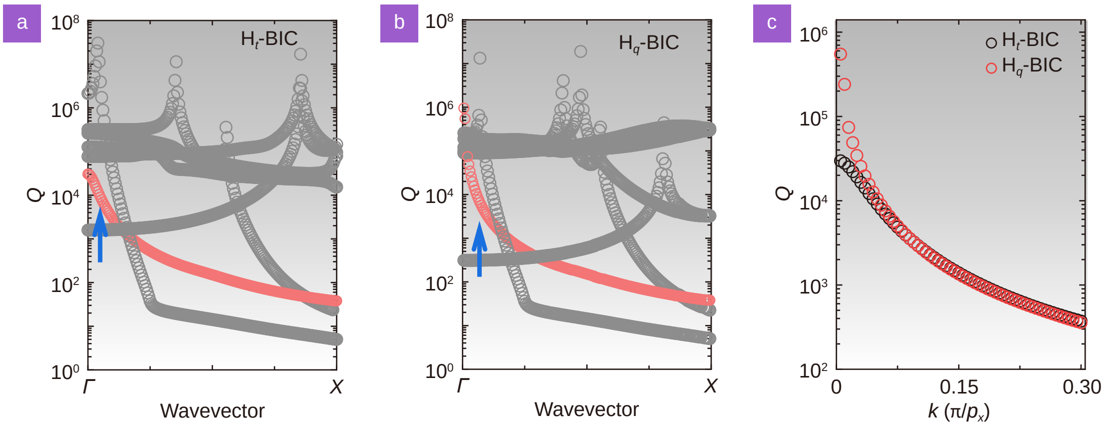

Fig. S4 | Radiative quality factors of H_t-BIC and H_q-BIC supercells. (**a, b**) Radiative quality factor of H_t-BIC and H_q-BIC supercells. (**c**) Radiative quality factors of the original U-qBIC band marked by the blue arrow with an asymmetry degree of 2.97%.

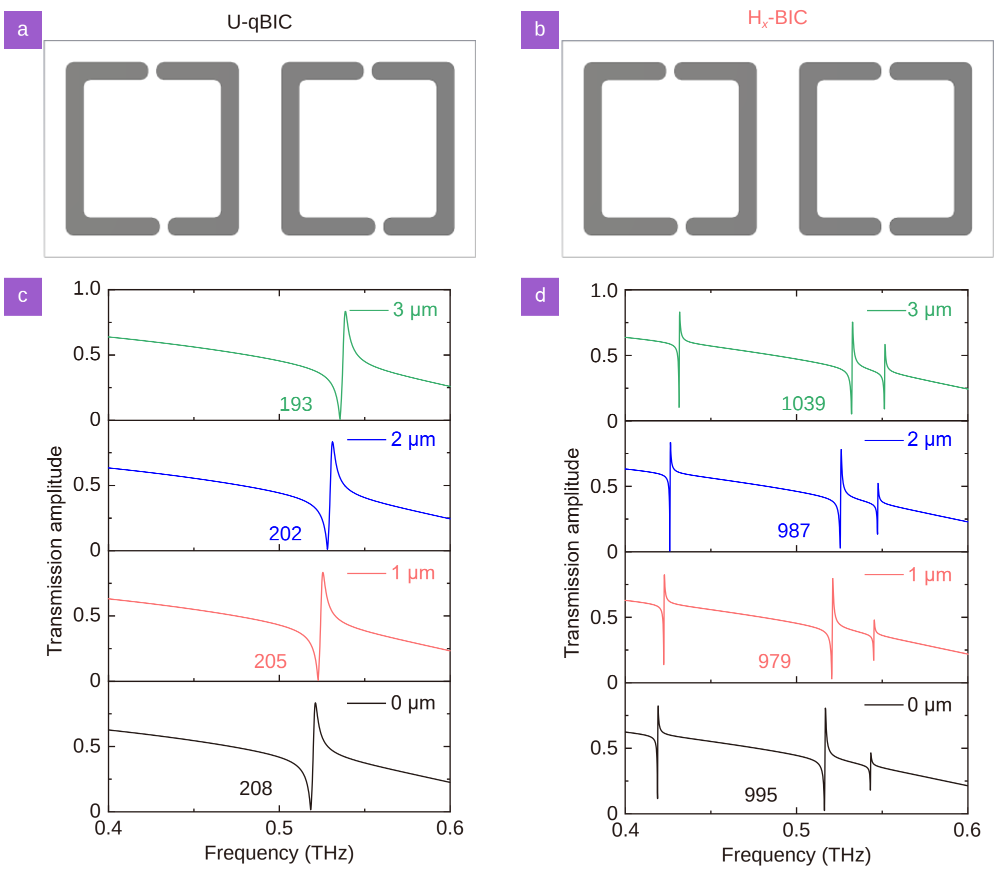

Fig. S5 | Resonances with fabrication imperfection. (**a, b**) Schematic diagram of U-qBIC and H_x-BIC supercells with a manufacturing imperfection defined as radius *r* (*r* = 3 μm). (**c, d)** Simulated transmission amplitude spectra and quality factors at different *r*.

References

S1. Han S, Gupta M, Cong LQ, Srivastava YK, Singh R. Toroidal and magnetic Fano resonances in planar THz metamaterials. *J Appl Phys* **122**, 113105 (2017).